Brain Stimulation 19 (2026) 103065

Contents lists available at ScienceDirect

Brain Stimulation

journal homepage: www.journals.elsevier.com/brain-stimulation

Real-time brain-computer interface control of walking exoskeleton with bilateral sensory feedback

Jeffrey Lim [a,1], Po T. Wang [a,1], Won Joon Sohn [b,c,2], Derrick Lin [c], Shravan Thaploo [a], Luke Bashford [h,3], David A. Bjanes [f], Angelica Nguyen [d], Hui Gong [d], Michelle Armacost [d], Susan J. Shaw [d], Spencer Kellis [k,3], Brian Lee [e,i,j], Darrin J. Lee [e,i,j], Payam Heydari [a,g], Richard A. Andersen [f], Zoran Nenadic [a,g,***], Charles Y. Liu [e,i,j,**], An H. Do [c,*]

[a] Department of Biomedical Engineering, University of California, Irvine (UCI), Irvine, CA, USA
[b] Abbott Laboratories, Plano, TX, USA
[c] Department of Neurology, UCI School of Medicine, Orange, CA, USA
[d] Department of Neurology, Rancho Los Amigos National Rehabilitation Center, Downey, CA, USA
[e] University of Southern California (USC) Neurorestoration Center, Keck School of Medicine of USC, Los Angeles, CA, USA
[f] Division of Biology and Biological Engineering, California Institute of Technology (Caltech), Pasadena, CA, USA
[g] Department of Electrical Engineering and Computer Science, UCI, Irvine, CA, USA
[h] Faculty of Medical Science, Newcastle University, UK
[i] Department of Neurosurgery, Rancho Los Amigos National Rehabilitation Center, Downey, CA, USA
[j] Department of Neurosurgery, Keck School of Medicine of USC, Los Angeles, CA, USA
[k] Blackrock Neurotech, Salt Lake City, UT, USA

ARTICLE INFO

Keywords:
Brain-computer interface
Bidirectional brain-computer interface
Electrocorticography
Direct cortical electrical stimulation
Spinal cord injury

ABSTRACT

Purpose: Brain–computer interfaces (BCIs) offer a pathway to restore ambulation in individuals with spinal cord injury (SCI). However, existing BCI systems for gait are unidirectional and lack sensory feedback. This study aimed to demonstrate that a bidirectional brain–computer interface (BDBCI) can simultaneously enable real-time brain-controlled walking and artificial leg sensation via electrical stimulation of the sensory cortex.

Methods: Epilepsy patients undergoing bilateral interhemispheric subdural electrocorticography (ECoG) implantation were recruited for this proof-of-concept study. Motor mapping identified electrodes in the leg motor cortex for decoding stepping intent, while sensory stimulation mapping determined stimulation sites in the somatosensory cortex to elicit artificial leg percepts. A custom embedded BDBCI decoded motor intent in real time to actuate a robotic gait exoskeleton (RGE) from ECoG signals and delivered leg swing sensory feedback via direct cortical stimulation. Performance was assessed through correlations between cued and decoded states, sensory reliability tasks, and control experiments.

Results: One subject was recruited and achieved a high decoding performance ($\rho = 0.92 \pm 0.04$, lag of 3.5 ± 0.5 s) across 10 runs of operating the BDBCI-controlled RGE. Bilateral leg percepts were validated through a blind step-counting task (92.8% accuracy, $p < 10^{-6}$). Control experiments verified that decoding was not affected by stimulation artifacts. No adverse events were reported.

Discussion: This study establishes the feasibility of an embedded system BDBCI for restoring both motor control and artificial sensation of walking. Leveraging interhemispheric leg sensorimotor cortices is safe and yields superior decoding compared to prior lateral brain convexity approaches. These findings provide a foundation for translating BDBCI technology into fully implantable systems for SCI patients with paraplegia.

* Corresponding author.
** Corresponding author. University of Southern California (USC) Neurorestoration Center, Keck School of Medicine of USC, Los Angeles, CA, USA.
*** Corresponding author. Department of Biomedical Engineering, University of California, Irvine (UCI), Irvine, CA, USA.
E-mail addresses: znenadic@uci.edu (Z. Nenadic), cliu@usc.edu (C.Y. Liu), and@uci.edu (A.H. Do).
[1] These authors contributed equally to this work.
[2] Work done while at Department of Neurology, UCI School of Medicine, Orange, CA, USA.
[3] Work done while at Division of Biology and Biological Engineering, California Institute of Technology (Caltech), Pasadena, CA, USA.

https://doi.org/10.1016/j.brs.2026.103065
Received 4 December 2025; Received in revised form 22 February 2026; Accepted 23 February 2026
Available online 28 February 2026

1. Introduction

Individuals with paraplegia due to spinal cord injury (SCI) typically experience a loss of lower extremity motor and sensory function. This often results in severe gait impairment and a dependence on wheelchairs, which increases the risk of other comorbidities such as heart disease, osteoporosis, and/or pressure ulcers [1]. These individuals typically rate the recovery of ambulatory function highly among their rehabilitation priorities [2–4]. Physical therapy is the current clinical standard of care and provides limited recovery [1]. Robotic gait exoskeletons emerged as a new standard in restoring gait after SCI, but are manually controlled and provide no sensory feedback. Recently, spinal cord stimulation (SCS) [5] has demonstrated a dramatic ability to restore motor, sensory, and autonomic function in people with SCI. However, this is typically only achieved in SCI recipients with more preserved function (i.e., ASIA C/D). More severely affected SCI recipients (i.e., ASIA A/B) have a $<5\%$ chance of regaining independent walking [6–11]. The combination of an electrocorticography (ECoG)--based brain-computer interface (BCI) and SCS [12] provided some additional motor improvement over SCS alone, but was only tested in a single subject with significant retained motor function (ASIA C). As such, improved methods to restore gait and sensory function after SCI are still needed, especially for those with the most severe injuries.

BCI technology is one such method for restoring gait after severe SCI. BCIs can bypass the site of SCI by using signals from the primary motor cortex (M1) to control ambulation devices. This has been achieved by both non-invasive [13,14] and invasive BCIs [15]. Notably, the motor aspect of walking after SCI has received significant attention in BCI research, overshadowing the restoration of sensation. Although motor restoration without sensory function is possible, it is highly suboptimal given the critical role of sensation in normal gait. For example, while gait restoration with leg prostheses, such as with RGEs, can be achieved without sensory feedback, it is well known that sensory impairment reduces gait velocity [16,17] and increases fall risk [18–20]. To address this, a bidirectional BCI (BDBCI) for ambulation could potentially elicit artificial leg sensation during BCI-controlled walking via direct cortical electrostimulation (DCES) of the primary somatosensory cortex (S1) [21–23], thereby restoring the able-bodied-like motor-sensory loop. However, such BDBCIs have yet to be demonstrated in SCI subjects; only unidirectional, invasive, ECoG-based BCIs controlling a robotic gait exoskeleton (RGE) exist [15]. Specifically, BDBCIs for walking with leg sensory feedback have not advanced beyond a highly limited feasibility demonstration in able-bodied individuals [24].

While the above examples indicate that restoring brain-controlled ambulation with leg sensory feedback in paraplegic SCI subjects is possible, existing BCI and BDBCI technologies for walking still face several shortcomings. First, in both of the ECoG-based BCI examples above [15,24], the decoding performances were inferior to that achieved by an EEG-based BCI for walking [13]. This is likely attributed to the fact that both studies utilized signals from the lateral M1. This area predominantly represents the upper extremities and only has limited lower-extremity motor representation compared to the robust leg representation in the interhemispheric leg M1 area [25]. Although the interhemispheric leg area is difficult to access surgically, it is likely optimal for invasive BCIs for walking and allows the delivery of artificial leg sensation. Finally, existing BCI systems typically rely on external computers to perform computationally intensive tasks, e.g., motor decoding. Such constant reliance wirelessly tethers the BCI to external systems and limits their practicality and energy efficiency in mobile applications. Instead, an embedded systems design approach where all functions are executed on board, would allow future BDBCIs to be highly compact, fully independent, and fully implantable systems. However, even though the BDBCI system in Ref. [24] leveraged an embedded system approach to achieve leg percepts during BCI operation, it only involved unilateral sensory feedback. Motivated by these outstanding problems, the current work demonstrates the feasibility of a BDBCI-RGE system for bilateral motor and sensory restoration of ambulation by utilizing bilateral interhemispheric ECoG implants. Real-time, bilateral sensorimotor functions were achieved using an embedded systems approach that served as a benchtop analogue to a fully-implantable BDBCI. This functionality was safely demonstrated 3 weeks post-implantation in an able-bodied epilepsy subject with bilateral interhemispheric ECoG grids, and high performance was rapidly established over the course of 9 days.

2. Methods

2.1. Study design and participants

This study seeks to demonstrate that an ECoG-based BDBCI can enable both brain-controlled RGE stepping and elicit artificial leg sensation (via S1 DCES in response to RGE stepping) without disrupting BCI control. Adults (age$>$18) undergoing Phase II epilepsy evaluation with subdural ECoG over M1/S1 were recruited. Exclusions were neurological comorbidities beyond epilepsy or medical conditions precluding safe participation. Implant locations were determined solely by clinical needs. Research occurred during the ICU admission. Any DCES was performed only after clinical monitoring ended and anti-seizure medications were resumed.

2.2. BDBCI–RGE system overview

The portable BDBCI system comprises a custom PCB, an FDA-cleared powered RGE (Ekso GT, Ekso Bionics, San Rafael, CA), and a custom RGE Interface (Fig. 1a). The BDBCI connects to 1.5 mm touch-proof ECoG leads, performs onboard motor decoding, S1 stimulation, and communicates over the MedRadio band (~406 MHz). A base station facilitates system configuration and data logging but is not required for online operation. The RGE Interface converts BDBCI MOVE commands into step actuation and reports left/right leg swings to trigger contralateral S1 stimulation.

2.3. BDBCI hardware

Three 48 MHz microcontrollers (Microchip Technology, Chandler, AZ) jointly execute all BDBCI tasks, including neural acquisition, real-time decoding, stimulation, and wireless communications. An amplifier/digitizer array (Intan, Intan Technologies, Santa Monica, CA) acquires up to 32 channels (plus reference/ground) at 500 Hz (16-bit). The programmable stimulator (charge pump cascade, programmable current source, and H-bridge) delivered biphasic, current-controlled trains up to 12 mA, 300 Hz, 250 μs/phase [26], with charge restriction $\leq$30 μC/cm^2/phase [27], and active charge balancing facilitated by onboard sensing [26]. Two MedRadio-band transceivers facilitate wireless communications with the base station and RGE Interface. Power was supplied by a 3.7 V, 2500 mAh Li-polymer battery.

2.4. Base-station software

A custom Windows C# user interface (UI) [26,28] on the base station was used for configuring BDBCI training (epochs/duration) and online decoding parameters (i.e., state transition thresholds), setting stimulation parameters per leg (current, frequency, pulse width, duration), delivering manually triggered stimulation, and logging cues/decoded outputs/timestamps for performance analysis. Note that online decoding and stimulation ran onboard the embedded BDBCI.

2.5. RGE interface

The RGE Interface consists of a microcontroller board interfaced with a MedRadio wireless transceiver, microphone, servo/cantilever, and two RGE ankle-mounted IMUs. The servo/cantilever was attached to the

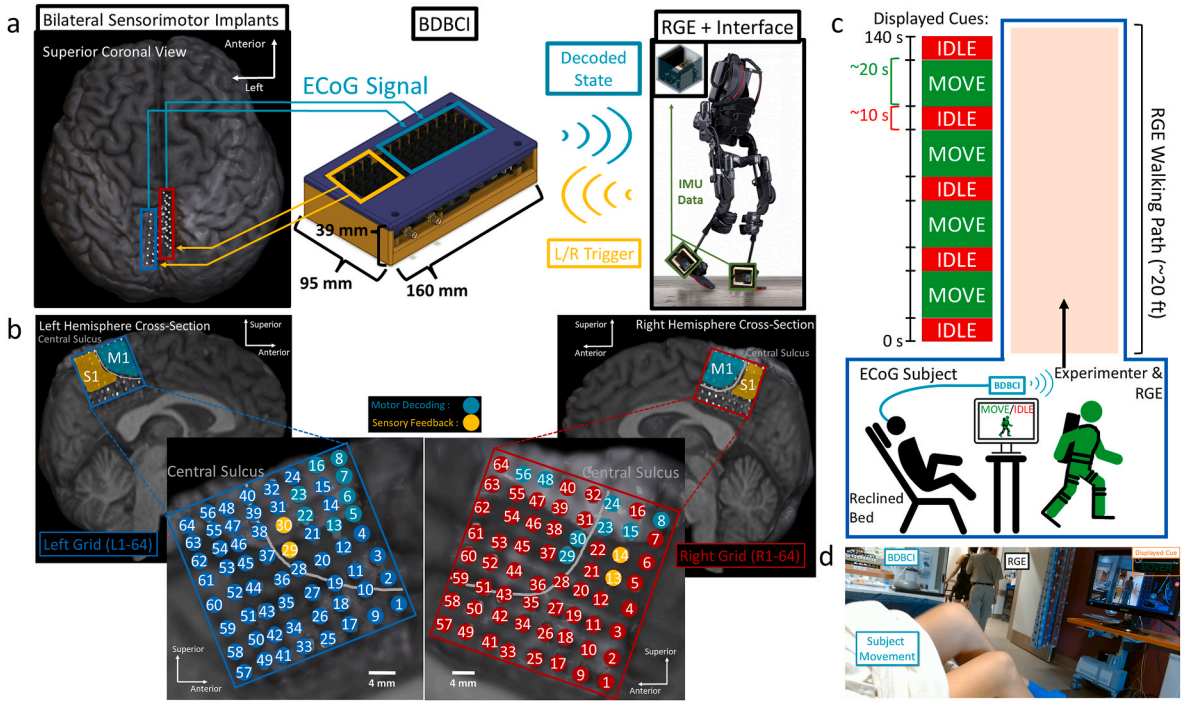

Fig. 1. **a**: BDBCI–RGE system. ECoG signals are decoded onboard to wirelessly control the RGE. The RGE Interface detects left/right leg swing and commands the BDBCI stimulator to elicit the corresponding percept via DCES. **b**: Co-registration of post-implant CT electrodes onto a 3D render of the post-implant MRI. Teal: decoding electrodes; Yellow: stimulation. **c**: Task schematic: the seated subject alternates IDLE/MOVE to control the RGE worn by an experimenter; RGE leg swings trigger contralateral S1 stimulation. **d**: Photograph of the setup.

RGE controller and depressed the step button upon command from the BDBCI. The RGE Interface records the IMU angular velocity, detects onset/offset of left/right swings using a threshold approach, and signals the BDBCI to deliver contralateral percepts during swing. At each completed step, the RGE emits an audio tone, which was captured by the microphone to inform the RGE Interface that another step could be initiated. This setup avoids modifying the RGE, preserves all regulatory-approved safety features, and allows an experimenter to quickly disable the RGE Interface if necessary.

2.6. CT–MRI co-registration

Post-implant CT (contacts) and MRI (anatomy) were co-registered using MATLAB [29,30] and Elastix [31,32] to localize interhemispheric leg M1/S1 (Fig. 1b).

2.7. Motor mapping and electrode selection

To enable brain-controlled walking, we first mapped the M1 region to identify channels exhibiting ECoG signal modulation corresponding to lower extremity movement. The subject performed stepping leg movements in the ICU bed (seated configuration) while ECoG data were acquired using the clinical amplifier array (Natus® Quantum™, Natus Medical Incorporated, Pleasanton, CA, USA, 512 Hz sampling rate). During this task, the subject alternated between 10 s IDLE/MOVE (seated bilateral marching) epochs. Channels on both interhemispheric grids were screened for modulation in common physiological EEG bands, including μ (8–12 Hz), β (12–25 Hz), high-β (30–50 Hz), and γ (80–160 Hz). Channels exhibiting robust γ synchronization and/or μ or β desynchronization were selected for decoder training (see Section 2.9). Unstable or artifact-laden channels were also excluded.

2.8. Sensory mapping

To enable sensory feedback during BDBCI operation, we relied on clinical cortical mapping which stimulated adjacent electrode pairs with current escalation (up to 20 mA) at 50 Hz, 2 s, and 250 μs pulse width to identify leg percepts (Natus® Nicolet™ Cortical Stimulator, Natus Medical Incorporated). We then re-verified these percepts with the BDBCI stimulator and systematically explored additional stimulation parameters not tested by the clinical mapping (pulse frequencies from 100 to 300 Hz and current amplitudes from 1.61 to 10.86 mA). The phase width was fixed at 250 μs and the total stimulation duration at 2 s. The mapping space was restricted to channels exhibiting sensory responses during clinical cortical mapping (primarily the superior half of each grid; see Supplement Section 3). After each stimulation, the subject reported the sensation quality and location. One contralateral electrode pair and parameter set per leg was chosen for subsequent testing, and reliability was assessed using the following blind step counting and blind sensory discrimination tasks.

In the blind step counting task, an experimenter wore a thigh-mounted IMU that triggered one percept per step. In 14 10-s trials per leg, the experimenter walked 2–8 steps out of subjects' view and hearing. The subject reported counts with a hand counter and feedback was given only after testing. Accuracy was compared to 10^6 Monte Carlo simulations. The empirical p-value was the fraction of simulations matching the subject's correct trials.

In the blind sensory discrimination task, a randomized list of 25 left leg percepts, 25 right leg percepts, and 25 null stimulation events (null stimulation involved parameters without any response during mapping) was delivered. After each stimulus, subjects identified the percept (left/right/null) they experienced without feedback. The accuracy of the subjects' response was compared with 10^6 Monte Carlo permutations to derive an empirical p-value.

2.9. Decoder training

Before online operation, the BDBCI collected 300 s of alternating 10 s IDLE/MOVE using mapped channels during seated marching. The BDBCI stored raw ECoG windows in memory and computed state-

specific feature extraction matrices.

2.10. Decoder architecture

The BDBCI's state decoder was developed similarly to our prior work in Ref. [28]. It facilitates subjects' brain control of RGE stepping by translating their ECoG signals to machine commands for the RGE. Briefly, the decoder preprocessed each window of 32-channel real-time ECoG data by the common average re-referencing and calculating the average power in the two bands. To reduce the dimensionality of the data, $d \in \mathbb{R}^{64}$ (32 channels, 2 bands), and enhance the class-separability, a 1D feature $f \in \mathbb{R}$ was extracted. Formally, $f = T_{\mathrm{LDA}}\Phi_{\mathrm{cPCA}}(d)$, where $\Phi_{\mathrm{cPCA}} : \mathbb{R}^{64} \rightarrow \mathbb{R}^{m}$ is the cPCA mapping with the intermediate dimension, m, determined by an eigenvalue criterion [33], and $T_{\mathrm{LDA}} \in \mathbb{R}^{1\times m}$ is the LDA feature extraction matrix. Due to cPCA's piecewise linear nature, each ECoG data window was projected onto two 1D subspaces: one principally informed by the MOVE state and the other principally informed by the IDLE state.

The parameters of a linear Bayesian classifier (class-conditional likelihoods modeled as Gaussians with pooled variances) were then estimated offline from the training data, with $P_I(M|f)$ and $P_M(M|f)$ being the posterior probability of walking based on the features in the IDLE and MOVE subspace, respectively. Note that $P_I(I|f) = 1 - P_I(M|f)$ and $P_M(I|f) = 1 - P_M(M|f)$. Subsequently, a real-time data window was transformed into a feature, f^*, and the overall posterior probability $P(M|f^*)$ was estimated from the subspace with the highest posterior probability ratio.

To determine the decoded state from $P(M|f^*)$, a binary state machine governed the transitions between the MOVE and IDLE states (illustrated in Fig. 2). When $P(M|f^*)$ exceeded the MOVE threshold (T_M), the decoded state transitioned from IDLE to MOVE state. When $P(M|f^*) < T_I$, the state transitioned from MOVE to IDLE state. Finally, when $T_I \leq P(M|f^*) \leq T_M$, the decoder remained in the current state.

2.11. Online calibration

A 10-fold cross-validation was used to estimate the offline decoding model's performance. Default transition thresholds were set at $T_M = 0.6$ and $T_I = 0.4$ and then calibrated online by recording posterior probabilities ($P(M|f^*)$) during alternating cue runs without RGE control or stimulation. The 90th and 10th percentiles of these distributions were used to update T_M and T_I, respectively. This calibration process was typically repeated for at least 5 iterations to finalize threshold values. If decoding performance fell below $\rho < 0.85$ offline or online, training was repeated and the selected channel set adjusted as needed.

2.12. Online BDBCI validation

Once the decoding model was calibrated, subjects proceeded to online BDBCI–RGE operation. Here, ECoG signals underlying bilateral stepping-like movements in bed were used to control RGE stepping, and visual and artificial sensory feedback provided for each step (Fig. 1d). The BD-BCI processed 750 ms windows online, and decoded MOVE states triggered steps via the RGE Interface. Stimulation parameters for left and right leg percepts (Section 2.8) were triggered by the corresponding RGE leg swings. For safety, an experimenter wore the RGE while the subject controlled it wirelessly from the hospital bed. Real-time operation utilized an interleaved decoding motif (Fig. 3), where ECoG acquisition paused during leg swings to avoid stimulation artifacts [30] and resumed after swing completion. Since the RGE cannot idle mid-step, the decoded state updated at the end of each step (MOVE: step again, IDLE: stand still). Decoding performance (ρ) was assessed as the lag-optimized Pearson correlation between instructional cues and decoded states. Before combined BDBCI–RGE operation, the subject completed short cue-following runs with online decoding only (no RGE or stimulation) for familiarization. RGE leg kinematics were recorded with wearable motion capture (XSens Movella, Enschede, Netherlands) at 100 Hz.

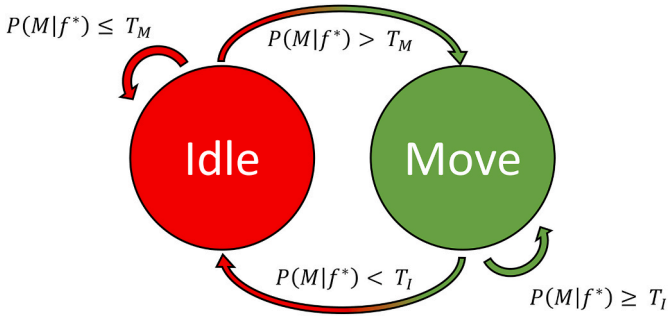

Fig. 2. Decoder state machine governing transitions between IDLE and MOVE based on posterior probability thresholds T_M and T_I.

2.13. Control experiments

To verify that BCI control was not driven by the effects of stimulation (i.e., decoder classifying electrical artifacts as motor cortex activation) or mirror motor neuron activity from observing the RGE, two control experiments were performed. In the first control experiment ("BCI-RGE"), the RGE control was enabled with real-time camera feedback, but stimulation was disabled. In the second control experiment ("BCI-Stimulation"), the RGE control and the subject's camera feedback were turned off, and the BDBCI automatically stimulated left and right leg percepts (2-s alternating epochs during MOVE state).

3. Results

3.1. Subject and implantation

The Institutional Review Board (IRB) of University of California, Irvine and Rancho Los Amigos National Rehabilitation Center approved the study. One participant (female, 50 years old) was recruited for this study. The subject had two 8 × 8 high-density ECoG grids (PMT; 2 mm diameter, 4 mm pitch) implanted in the left and right interhemispheric fissures over leg M1/S1 (L1–64 and R1–64, electrode locations shown in Fig. 1b) over 19 days (research procedures occurred on days 11–19). Supplement Section 1 provides details on implantation methodology and clinical details.

3.2. Motor decoding model characteristics

During the motor mapping (Section 2.7 and 2.9), we identified localized ECoG high-β and γ bands contained salient associated with cyclic leg movements. This included robust high-β desynchronization and γ synchronization on several channels (Fig. 4). Supplement Fig. 1 shows a map of M1 channels that exhibit significant high-β and γ band modulation during seated leg movements based on the motor mapping procedure. The μ and β bands were excluded as the subject exhibited frequent random bursts within these bands unrelated to leg movements. These were interpreted as a normal variant of background rhythm (see Supplement Fig. 6 for examples of subject's ECoG signals). Fig. 4 shows decoder spatial weights and representative envelopes. For experimental expedience, the base station downloads training ECoG data from the BDBCI to generate the BCI decoding model (process is equivalent to the onboard model generation [28]), which is then uploaded to the BDBCI. To optimize the BDBCI decoding performance, only a subset of 15 electrodes (Fig. 1b) exhibiting robust motor-related modulation in the high-β (30–50 Hz) and γ (80–160 Hz) bands (Fig. 4) were ultimately chosen for the BDBCI-RGE task.

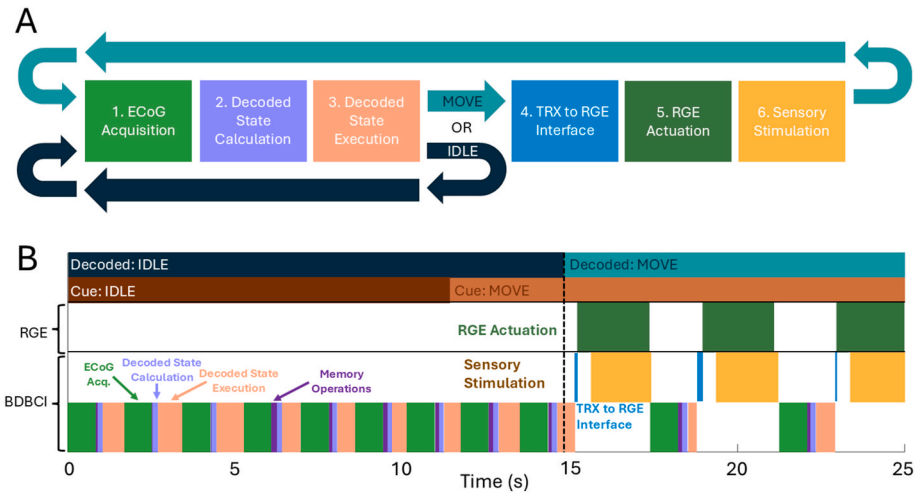

Fig. 3. **A**: Online sequence for acquisition, decoding, actuation, and stimulation. **B**: Example timing diagram from a BDBCI-RGE run illustrating an IDLE-to-MOVE state transition. Inter-leaved actuation/stimulation is depicted during the MOVE state.

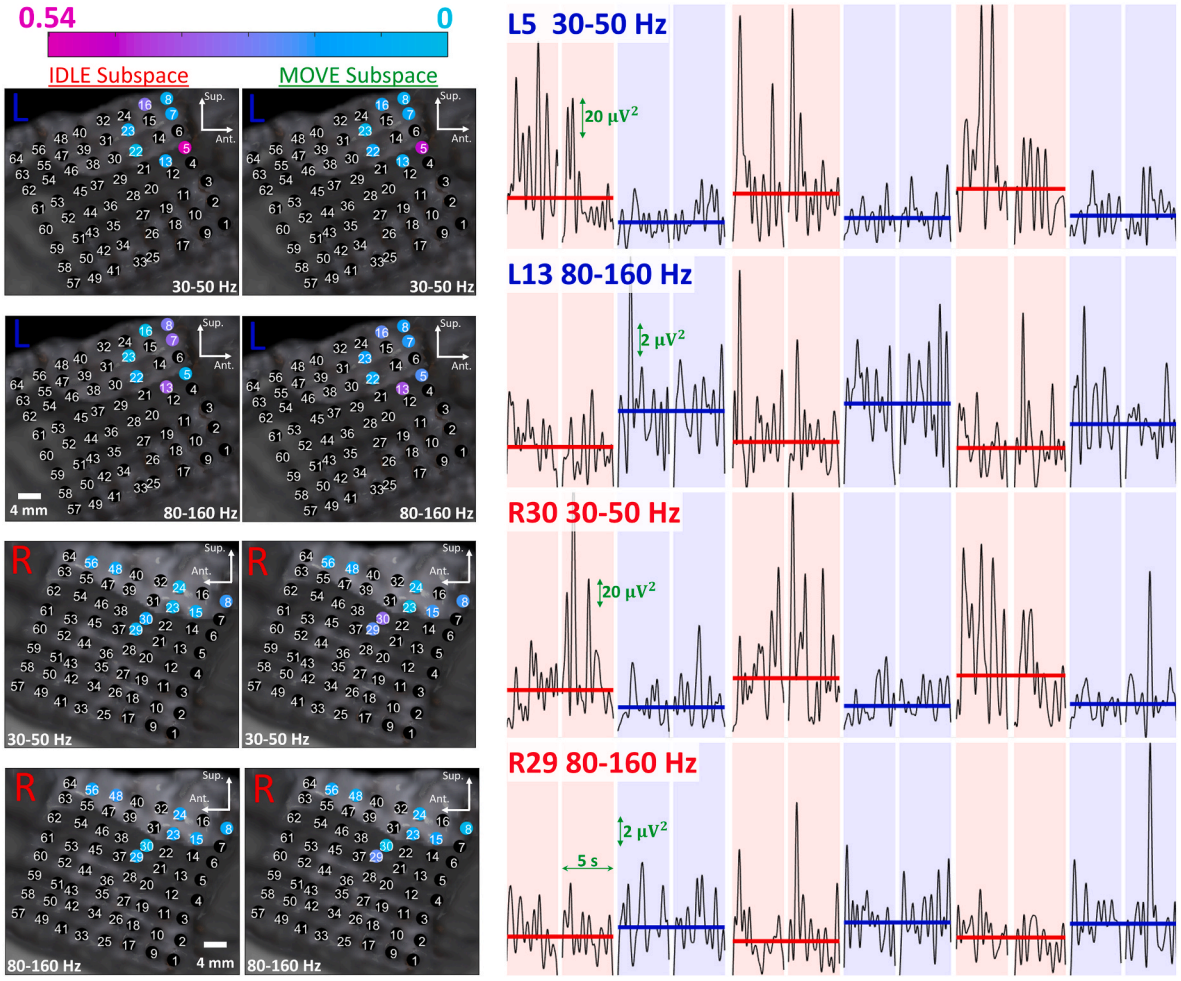

Fig. 4. **Left:** Spatial weights of motor decoding model mapped to locations of corresponding coregistered ECoG electrodes in the left and right interhemispheric grids. Warmer colors indicate electrodes containing relevant decoding features for the given frequency band (high-β or γ), whereas cooler colors indicate electrodes that were less relevant for decoding. **Right:** Time-domain power envelopes from a subset of training data in the electrodes with the strongest decoder weights (two electrodes are shown from each side). *Red and blue shades:* IDLE and MOVE states, respectively. *Red and blue horizontal bars:* median band powers in each state. White gaps represent brief discontinuities between recording epochs, where no data were acquired. The γ power synchronization occurs during the MOVE state (i.e., red shade compared to blue shade). Conversely, high-β power desynchronizes during the MOVE state.

3.3. Sensory mapping and validation

Sensory mapping was performed (full responses in Supplement Tables 1 and 2). Ultimately, we chose channel L29–30 (Figs. 1 b), 8.22 mA, 100 Hz for the right-leg percept (posterior lower leg to heel tingling), and channel R13–14, 3.80 mA, 300 Hz for the left-leg percept (posterior lower leg tingling). These were validated with the blind step counting task, where the subject correctly counted the steps taken in 100% and 86% of right/left leg trials, respectively (empirical p-value $< 10^{-6}$). In the blind sensory discrimination task, the subject identified 96%, 84%, and 100% of right leg, left leg, and null percepts, respectively (empirical p-value $< 10^{-6}$). See Supplement Section 4 for sensory task validation from additional subjects.

3.4. Online familiarization performance

Across 5 runs (~4–5 min each; 20–25 min total), the subject achieved mean online performance of $\rho = 0.89 \pm 0.06$ with lag 2.2 ± 0.4 s while following alternating walk/idle cues without RGE control or stimulation.

3.5. BDBCI–RGE online control with sensory feedback

After both motor decoding and artificial sensory feedback established, the subject performed 5 runs/day over 2 days (~2.5 min/run; ~25 min total). Mean performance was $\rho = 0.92 \pm 0.04$ with lag 3.5 ± 0.5 s (Day 1: $\rho = 0.89 \pm 0.02$, lag 3.4 ± 0.5 s; Day 2: $\rho = 0.94 \pm 0.03$, lag 3.6 ± 0.5 s). Performance of a representative run is shown in Fig. 6 and Supplementary Video (see Supplement, Section 5 for performance metrics for all individual runs). For each cue change, state transitions occurred within 1–2 decoding windows (1.8–3.8 s) with high accuracy. The subject confirmed in all 10 runs that RGE steps triggered matching contralateral leg percepts and reported that sensation aided task performance. With ~2.5 s steps and ~1 s decoding windows, the nominal decoding rate was ~0.29 Hz during stepping and ~1 Hz while idle. The BCI decoding performance results for all experimental conditions are summarized in Fig. 5.

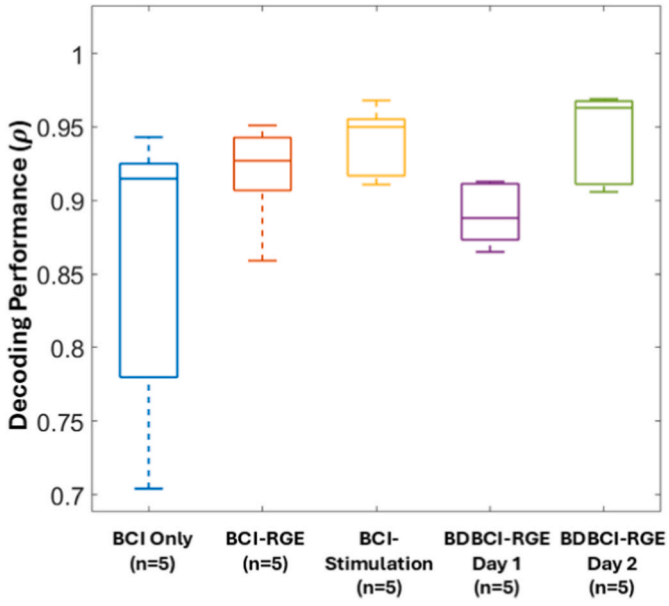

Fig. 5. Box-and-whisker plot of median BCI decoding performance across all experimental and control conditions (box: upper and lower 25th percentile; whiskers: maximum and minimum). No significant difference existed between any condition and the BDBCI-RGE condition.

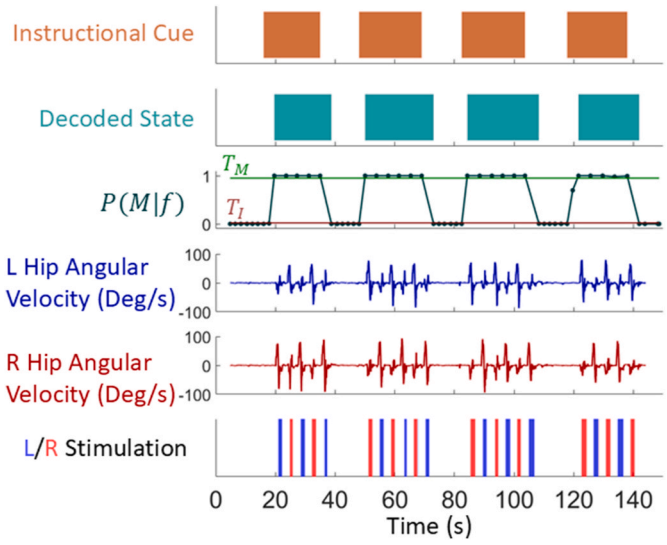

Fig. 6. Representative BDBCI–RGE online run. **Instructional Cue**: Orange blocks represent MOVE cues. **Decoded State**: Teal represents decoded MOVE states. $P(M|f)$ denotes MOVE probability for each window (dots); T_M/T_I are transition thresholds. When decoding MOVE, the RGE steps, as indicated by **L/R Hip Angular Velocity**. **L/R stimulation** shows periods of contralateral S1 stimulation corresponding to RGE leg swings.

3.6. Control experiments

Performance for the *BCI–RGE task* (RGE control on, DCES off) was $\rho = 0.93 \pm 0.01$, lag 3.6 ± 0.9 s. Performance for the *BCI–Stimulation task* (no RGE control, automatic cycling between left/right leg percept DCES during MOVE) was $\rho = 0.94 \pm 0.02$, lag 3.8 ± 0.4 s. Both were comparable to BDBCI–RGE (two-sided Wilcoxon rank sum, $p = 0.75$ and $p = 0.27$, respectively), indicating decoding was driven by intended M1 activity rather than artifacts or mirror motor neuron activity.

3.7. Safety

No adverse events occurred. In particular, no seizures were induced during cortical mapping, sensory tasks, or BDBCI procedures. Channels R52–53, R53–54, and R55–56 elicited pain percepts during clinical mapping and were avoided during BDBCI sensory mapping.

4. Discussion

Herein we described a BDBCI-RGE system that enabled real-time brain-controlled walking and provided bilateral artificial leg sensory feedback. This was safely achieved in a subject with ECoG implantation in the bilateral interhemispheric leg M1 area, and with high decoding performance. Furthermore, sensory leg percepts were consistent, repeatable, and did not interfere with the BDBCI performance. The high accuracy of identifying steps during the blind step counting task indicates that the contralateral S1 stimulation triggered by BDBCI-RGE steps conveyed step-based sensory information with gait-phase resolution (i.e., stimulation during swing, no stimulation during stance). Finally, this was achieved with the entire BDBCI implemented on a portable embedded form factor without compromising overall function.

Whereas our prior work [24] demonstrated a BDBCI-RGE utilizing ECoG grids implanted on the lateral convexity M1, the current work represents the first implementation of a BDBCI for walking that incorporates bilateral inter-hemispheric leg sensorimotor areas. Our current work achieved a high performance (ρ up to 0.97, overall average ρ of 0.92) over a short period of time (~9 days). This represents a marked decoding performance increase compared to Ref. [24] (ρ of 0.80). This difference in performance may be attributed to a more direct coverage of

the leg M1 area in the interhemispheric space. The leg M1 area likely provides more robust and reliable localized ECoG modulation associated with leg movements. Furthermore, the BCI performance using signals from the lateral M1 convexity [15,24] was inferior to that achieved by an EEG-based BCI [13], which reinforces the notion that the interhemispheric region is likely the most optimal recording site for BCI-walking applications. Finally, although interhemispheric ECoG implants are uncommon and complex to perform, this study demonstrates interhemispheric ECoG implantation can be safely leveraged for invasive BDBCI systems.

DCES likely represents the safest and most optimal approach to elicit artificial leg sensation. Non-invasive approaches, including transcranial magnetic and electrical stimulation involves equipment that is too bulky and power hungry for ambulatory applications, or is too non-specific to elicit leg sensation. Alternatively, peripheral nervous system stimulation (as in Ref. [34]) will only work above the lesion in paraplegic and insensate SCI recipients. However, stimulation of the torso or upper extremity may result in confusion or competition for neural resources, as recipients would be forced to associate these "non-ecologic" sensory locations with leg swing. Finally, alternative invasive approaches as superlesional spinal cord stimulation [35] would require additional surgery, which would incur additional risks. Conversely, ECoG electrode arrays can often be implanted such that cortical coverage for S1 DCES and M1 motor control is achieved simultaneously (as in this work), thereby incurring no additional surgical risk. Furthermore, DCES may be capable of delivering rich sensory modalities (e.g., proprioception [36]) and long-term DCES has been shown to be safe in existing FDA-approved commercial devices (e.g., Neuropace [Neuropace, Mountain View, CA, USA]) and other large clinical trials [37].

Our BDBCI system is also the first to implement bilateral lower extremity artificial sensation alongside motor decoding in a single BDBCI-RGE system. By comparison, our work in Ref. [24] only involved unilateral sensory feedback. Beyond this report, there have been no other BDBCIs for gait and the lower extremities. The primary concern for employing DCES for sensory feedback is the risk of compromising the motor decoding, either through electrical artifacts [30,38] or evoked neural activity. We addressed these problems by interleaving motor decoding and stimulation processes. The results from our control experiments (Section 3.5) suggest that the BDBCI operation was driven by M1 ECoG activity underlying leg movement intent, and not by stimulation artifacts, evoked motor neuron activity, or mirror neuron activation. This approach is similar to that used in Ref. [39], which employed amplifier blanking to accomplish interleaving of acquisition and stimulation processes (see Supplement, Section 6 for example of artifact free ECoG signal during BDBCI operation with interleaving). However, interleaving approaches are suboptimal as they introduce discontinuities in decoding and delay BDBCI responses. The normal human sensorimotor loop requires constant simultaneous sensory feedback, which is not permitted by interleaving or blanking. Hence, this makes it difficult for users to appreciate critical gait events such as transitions to double support, gait perturbations, etc. This continues to be a problem in BDBCI technologies, and will require novel methods of real-time stimulation artifact elimination [40,41] to achieve "full duplex" capability.

Our BDBCI-RGE device achieved high performance with and without the artificial sensory feedback. Though BCI decoding performance showed no significant change with sensory feedback (as seen in the control experiments), it is possible that such feedback instead improves functional outcomes, particularly for future, insensate, paraplegic SCI users. More specifically, since sensory impairments reduce gait velocity [16,17] and increase fall risk [18–20], we therefore expect that artificial sensory feedback may facilitate improved functional and safety outcomes in these areas. Specifically, with respect to BDBCI-RGE operation, users may achieve faster gait velocity or reduced risk of falls by providing sensory confirmation of weight transfer and acceptance. Although not directly tested here, such a finding would be consistent with prior work [22,42] which showed that sensory feedback can improve functional outcomes in upper extremities neuroprosthesis application.

An important aspect of our BDBCI is that all functions are implemented as an embedded system within a compact footprint. While a base station computer was used, it was only required for setting parameters, initiating/aborting decoding functions, and logging experimental data. In particular, the BDBCI can operate entirely independently once configured and initialized via the base station computer. The portability of the entire system could be further improved by replacing the base station computer with a mobile device or tablet. Furthermore, the existing BDBCI form factor would allow it be readily mounted onto the RGE, and therefore enable applications where the subject (as opposed to an experimenter) is in the RGE. By comparison, other existing BDBCI systems such as [22,42], rely on large, rack-mounted, off-the-shelf systems, or are constantly tethered to external computers for signal processing, which limit their applicability in mobile applications. Although the current system is not yet implantable, the design lends itself to be translated into a fully implantable device (discussed below). When compared to existing implantable BCI walking applications as [12,15], a fully implantable incarnation of our BDBCI is expected to operate fully independently on rechargeable battery power. As such, improved mobility, power efficiency, and aesthetics could be achieved by eliminating the need for constant wireless streaming to a permanently tethered computing system and constant magnetic power induction from an external power source.

A limitation of this study is that it was only performed in 1 able-bodied epilepsy subject. However, this subject provided a unique opportunity, as the bilateral interhemispheric ECoG implants used here for Phase 2 epilepsy surgery evaluations are extremely rare. An additional limitation is that the motor behavior used in this study was seated step-like movements instead of stepping while standing or actually walking. This leaves open the concern that the high BDBCI performance demonstrated here may not generalize to the paraplegic SCI population. For example, one concern in translating the BDBCI-RGE from able-bodied epilepsy subjects to SCI subjects is that ECoG modulation underlying walking intent may not be present or sufficient for BCI control. Though leg M1 behavior is generally assumed to be intact post-injury, it is possible that the neural circuitry has changed as a direct result of the injury or due to an extended period of disuse [43]. However, previous literature has indicated that this behavior can be retrained or reacquired by SCI subjects. For example, King et al. [44] demonstrated the ability for a SCI subject to control an EEG-based BCI connected to lower-extremity FES. Although the subject initially had a low degree of control over the BCI due to inadequate EEG motor-related modulation, the subject was eventually able to achieve extremely high performance in BCI-controlled walking after 21 weeks. Similarly, Benabid et al. [15] and Lorach et al. [12] demonstrate the ability for SCI subjects to operate BCI gait systems 1–2 years post-implantation using signals from the M1 lateral convexity area. The decoding performance analysis showed a maximal correlation at a lag of ~3.5 s. Much of this lag can be attributed to the slow RGE stepping rate, slow physiological response of high-β band signals, and (to a lesser extent) delays in data processing and wireless transmission. However, this latency is commensurate to the 0.29 Hz step rate of the RGE. Nevertheless, future BDBCI-RGE walking will likely need to have lower latency, and this can be achieved by increasing the RGE step rate/speed and by limiting the BDBCI to only using high-γ as the input signal (known for its high temporal coupling with motor behavior [45] and stepping [25]). Future work will need to directly address the above limitations by implanting the BDBCI device in the target SCI population. In addition, since the subject's ability to distinguish gait phase information was inferred in this study through the blind step counting task and the fact that stimulation is only delivered during the swing phase of the BD-BCI RGE task, future studies will need to directly assess subjects' perception and sensory-motor integration of gait phase specific artificial sensory information (e.g., via formal

psychophysical or functional metrics). Anecdotally, our BDBCI-RGE system has received an FDA IDE to proceed with such investigations.

Ultimately, we envision a fully implantable version of our device, which was previously described in [26]. Briefly, a skull-implanted unit interfaces with ECoG electrodes placed over M1/S1, and performs signal acquisition and stimulation channel selection. This skull unit is connected to a chest-wall implanted unit via a subcutaneous tunneling cable. The chest unit contains electronic components to perform all BDBCI functions, including signal processing, generation of electrical stimulation pulses, and wireless communication with the base station and end effector units. Such a fully-implantable BDBCI would facilitate chronic implantation in future paraplegic SCI recipients without the need for any transdermal components that could pose infection risks. The work presented here serves as an important foundation for the advancement of BDBCI technology towards such a fully implantable system, which may in turn present new avenues for treating sensorimotor deficits in affected patient populations. However, miniaturization of the BDBCI system is necessary for full implantability. We expect the BDBCI to be implementable with a footprint comparable to that of existing implantable neural devices (e.g., NeuroPace RNS® system: 60 × 27.5mm, Medtronic Percept™ PC neurostimulator: 68 × 51 mm). A unidirectional version of our system [28] already reached a similar size. Further applying advanced multilayer PCB design techniques, smaller surface-mounted components, and CMOS system-on-a-chip (SOC) integration of all electronic hardware components can drastically reduce the device footprint. For example, our earlier work showed that significant footprint and power reduction was achieved via CMOS integrated circuit implementation of an amplifier array and stimulator module [46–49]. However, more comprehensive SOC implementation and subsequent testing and validation are expensive. As such, SOC solutions are typically implemented only after the proof-of-concepts are thoroughly demonstrated.

Additional future directions may include providing sensory training to enhance the accuracy in sensory discrimination and detection in BDBCI operation, as well as addressing long-term challenges such as changes to artificial sensation due to habituation/adaptation to electrical stimulation. Other non-BDBCI sensory applications may also be implemented, such as skin ischemia-related warning percepts or bladder distension signals. Outside of neuroprosthesis applications, the BDBCI may also be able to utilize the neurorehabilitative effects of DCES. Inspired by prior work demonstrating that combining BCI and spinal cord stimulation provided rehabilitative benefits after SCI [12] the addition of sensory feedback to BCI-controlled spinal cord stimulation may activate novel Hebbian processes which could improve the recovery of function in damaged sensory pathways.

CRediT authorship contribution statement

Jeffrey Lim: Writing – original draft, Visualization, Validation, Software, Methodology, Investigation, Formal analysis, Data curation. **Po T. Wang:** Writing – review & editing, Writing – original draft, Visualization, Validation, Software, Resources, Project administration, Methodology, Investigation, Formal analysis, Data curation. **Won Joon Sohn:** Writing – review & editing, Software, Methodology, Investigation. **Derrick Lin:** Writing – review & editing, Validation, Software, Methodology, Investigation. **Shravan Thaploo:** Writing – review & editing, Methodology, Investigation. **Luke Bashford:** Writing – review & editing, Methodology, Investigation, Data curation. **David A. Bjanes:** Writing – review & editing, Methodology, Investigation, Data curation. **Angelica Nguyen:** Resources, Methodology, Investigation. **Hui Gong:** Writing – review & editing, Supervision, Investigation. **Michelle Armacost:** Writing – review & editing, Supervision, Investigation. **Susan J. Shaw:** Writing – review & editing, Supervision, Resources, Project administration, Investigation. **Spencer Kellis:** Writing – review & editing, Methodology, Investigation, Data curation, Conceptualization. **Brian Lee:** Writing – review & editing, Resources, Methodology. **Darrin J. Lee:** Writing – review & editing, Resources, Project administration, Methodology, Investigation. **Payam Heydari:** Writing – review & editing, Resources, Methodology, Funding acquisition, Conceptualization. **Richard A. Andersen:** Writing – review & editing, Supervision, Resources, Project administration, Methodology, Investigation, Funding acquisition, Conceptualization. **Zoran Nenadic:** Writing – review & editing, Supervision, Resources, Project administration, Methodology, Investigation, Funding acquisition, Formal analysis, Conceptualization. **Charles Y. Liu:** Writing – review & editing, Project administration, Investigation, Funding acquisition, Conceptualization, Methodology. **An H. Do:** Writing – review & editing, Writing – original draft, Validation, Supervision, Software, Resources, Project administration, Methodology, Investigation, Funding acquisition, Conceptualization.

Ethics statement

All studies were performed with the approval of the Institutional Review Boards of the University of California, Irvine and Rancho Los Amigos National Rehabilitation Center.

Funding

This work was supported by the National Science Foundation (NSF) Grant number 1646275.

Declaration of competing interest

The authors declare the following financial interests/personal relationships which may be considered aps potential competing interests:

- Drs. Do, Nenadic, Liu, Heydari, and Andersen jointly hold patents and grant funding from the US government directly related to the work presented here.
- Dr. Kellis currently works at Blackrock Neurotech, but the work was performed prior to his employment at Blackrock Neurotech.
- Dr. Sohn currently works at Abbott Laboratories, but the work was performed prior to his employment at Abbott Laboratories.

Appendix A. Supplementary data

Supplementary data to this article can be found online at https://doi.org/10.1016/j.brs.2026.103065.

References

[1] Johnson Renee L, Brooks CA, Whiteneck Gale G. Cost of traumatic spinal cord injury in a population-based registry. Spinal Cord August 1996;34(8):470–80. Number: 8 Publisher: Nature Publishing Group.
[2] Kim D Anderson. Targeting recovery: priorities of the spinal cord-injured population. J Neurotrauma 2004;21(10):1371–83. https://doi.org/10.1089/neu.2004.21.1371. _eprint.
[3] Collinger Jennifer L, Boninger Michael L, Bruns Tim M, Curley Kenneth, Wang Wei, Weber Douglas J. Functional priorities, assistive technology, and brain-computer interfaces after spinal cord injury. J Rehabil Res Dev April 2013;50(2):145–60.
[4] Lin Derrick, Tran Tracie, Thaploo Shravan, Matias Jose Gabrielle E, Pixley Joy E, Nenadic Zoran, Do An H. Perception of brain-computer interface implantation surgery for motor, sensory, and autonomic restoration in spinal cord injury and stroke. Front. Neurosci. 17 March 2026;20. https://doi.org/10.3389/fnins.2026.1678175. Sec. Neuroprosthetics.
[5] Reggie Edgerton Victor, Harkema Susan. Epidural stimulation of the spinal cord in spinal cord injury: current status and future challenges. Expert Rev Neurother 2011;11(10):1351–3.
[6] Rui Wan Kai, Ng Zhi Yan Valerie, Kwee Wee Seng, Fatimah Misbaah, Lui Wenli, Phua Min Wee, Qi Yue Rosa So, Maszczyk Tomasz Karol, Premchand Brian, Saffari Seyed Ehsan, et al. Recovery of volitional motor control and overground walking in participants with chronic clinically motor complete spinal cord injury: restoration of rehabilitative function with epidural spinal stimulation (restores) trial - a preliminary study. J Neurotrauma 2024.
[7] Kandhari Sachin, Sharma Dewaker, Samuel Sachin, Sharma Gaurav, Majumdar Pritam, Edgerton V Reggie, Gad Parag. Epidural spinal stimulation enables global sensorimotor and autonomic function recovery after complete

paralysis: 1 st study from India. IEEE Trans Neural Syst Rehabil Eng 2022;30:2052–9.
[8] Rejc Enrico, Angeli Claudia A, Bryant Nicole, Harkema Susan J. Effects of stand and step training with epidural stimulation on motor function for standing in chronic complete paraplegics. J Neurotrauma 2017;34(9):1787–802.
[9] Gill Megan L, Grahn Peter J, Calvert Jonathan S, Linde Margaux B, Lavrov Igor A, Strommen Jeffrey A, Beck Lisa A, Sayenko Dimitry G, Van Straaten Meegan G, Drubach Dina I, et al. Neuromodulation of lumbosacral spinal networks enables independent stepping after complete paraplegia. Nat Med 2018;24(11):1677.
[10] Wagner Fabien B, Mignardot Jean-Baptiste, Le Goff-Mignardot Camille G, Demesmaeker Robin, Komi Salif, Capogrosso Marco, Rowald Andreas, Seáñez Ismael, Caban Miroslav, Pirondini Elvira, et al. Targeted neurotechnology restores walking in humans with spinal cord injury. Nature 2018;563(7729):65–71.
[11] Rowald Andreas, Komi Salif, Demesmaeker Robin, Baaklini Edeny, Hernandez-Charpak Sergio Daniel, Paoles Edoardo, Montanaro Hazael, Cassara Antonino, Becce Fabio, Lloyd Bryn, et al. Activity-dependent spinal cord neuromodulation rapidly restores trunk and leg motor functions after complete paralysis. Nat Med 2022;28(2):260–71.
[12] Lorach Henri, Galvez Andrea, Spagnolo Valeria, Martel Felix, Karakas Serpil, Intering Nadine, Vat Molywan, Faivre Olivier, Harte Cathal, Komi Salif, Ravier Jimmy, Collin Thibault, Coquoz Laure, Sakr Icare, Baaklini Edeny, Hernandez-Charpak Sergio Daniel, Dumont Gregory, Buschman Rik, Buse Nicholas, Denison Tim, Nes Ilse van, Asboth Leonie, Watrin Anne, Struber Lucas, Sauter-Starace Fabien, Langar Lilia, Vincent Auboiroux, Carda Stefano, Chabardes Stephan, Aksenova Tetiana, Demesmaeker Robin, Charvet Guillaume, Bloch Jocelyne, Courtine Grégoire. Walking naturally after spinal cord injury using a brain–spine interface. Nature June 2023;618(7963):126–33. Number: 7963 Publisher: Nature Publishing Group.
[13] King Christine E, Wang Po T, McCrimmon Colin M, Chou Cathy CY, Do An H, Nenadic Zoran. Brain-computer interface driven functional electrical stimulation system for overground walking in spinal cord injury participant. In: 2014 36th annual international conference of the IEEE engineering in medicine and biology society; August 2014. p. 1238–42. ISSN: 1558-4615.
[14] Do An H, Wang Po T, King Christine E, Chun Sophia N, Nenadic Zoran. Brain-computer interface controlled robotic gait orthosis. J NeuroEng Rehabil 2013;10(1):1–9. Publisher: Springer.
[15] Louis Benabid Alim, Costecalde Thomas, Eliseyev Andrey, Charvet Guillaume, Verney Alexandre, Karakas Serpil, Foerster Michael, Lambert Aurélien, Morinière Boris, Abroug Neil, others. An exoskeleton controlled by an epidural wireless brain–machine interface in a tetraplegic patient: a proof-of-concept demonstration. Lancet Neurol 2019;18(12):1112–22. Publisher: Elsevier.
[16] Wuehr Max, Schniepp Roman, Schlick Cornelia, Huth Sabrina, Pradhan Cauchy, Dieterich Marianne, Brandt Thomas, Jahn Klaus. Sensory loss and walking speed related factors for gait alterations in patients with peripheral neuropathy. Gait Posture 2014;39(3):852–8.
[17] Lipsitz Lewis A, Manor Brad, Habtemariam Daniel, Iloputaife Ikechukwu, Zhou Junhong, Travison Thomas G. The pace and prognosis of peripheral sensory loss in advanced age: association with gait speed and falls. BMC Geriatr 2018;18(1):274.
[18] Khan Alia, Pujol Clara, Laylor Mark, Unic Nikola, Pakosh Maureen, Dawe Jaclyn, Musselman Kristin E. Falls after spinal cord injury: a systematic review and meta-analysis of incidence proportion and contributing factors. Spinal Cord 2019;57(7):526–39.
[19] Wilson Samuel J, Garner John C, Paul D Loprinzi. The influence of multiple sensory impairments on functional balance and difficulty with falls among us adults. Prev Med 2016;87:41–6.
[20] Musselman Kristin E, Arora Tarun, Chan Katherine, Alavinia Mohammad, Bone Mackenzie, Unger Janelle, Lanovaz Joel, Oates Alison. Evaluating intrinsic fall risk factors after incomplete spinal cord injury: distinguishing fallers from nonfallers. Archiv Rehabil Res Clin Trans 2021;3(1):100096.
[21] Hiremath SV, Tyler-Kabara EC, Wheeler JJ, Moran DW, Gaunt RA, Collinger JL, Foldes ST, Weber DJ, Chen W, , et alBoninger ML. Human perception of electrical stimulation on the surface of somatosensory cortex. PLoS One 2017;12(5):e0176020. Publisher: Public Library of Science.
[22] Flesher S, Downey J, Collinger JL, Foldes S, Weiss J, Tyler-Kabara E, Bensmaia S, Schwartz A, Boninger M, Gaunt R. Intracortical microstimulation as a feedback source for brain-computer interface users. Brain-Comput Interface Res 2017:43–54. Springer.
[23] Lee Brian, Kramer Daniel, Salas Michelle Armenta, Kellis Spencer, Brown David, Dobreva Tatyana, Klaes Christian, Heck Christi, Liu Charles, Andersen Richard A. Engineer-ing artificial somatosensation through cortical stimulation in humans. Front Syst Neurosci 2018;12:24. Publisher: Frontiers Media SA.
[24] Lim Jeffrey, Wang Po T, Sohn Won Joon, Serrano-Amenos Claudia, Ibrahim Mina, Lin Derrick, Thaploo Shravan, Shaw Susan J, Armacost Michelle, Gong Hui, et al. Early feasibility of an embedded bi-directional brain-computer interface for ambulation. In: 2024 46th annual international conference of the IEEE engineering in medicine and biology society (EMBC). IEEE; 2024. p. 1–5.
[25] McCrimmon CM, Wang PT, Heydari P, Nguyen A, Shaw SJ, Gong H, Chui LA, Liu CY, Nenadic Z, Do AH. Electrocorticographic encoding of human gait in the leg primary motor cortex. Cerebr Cortex 2018;28(8):2752–62. Publisher: Oxford University Press.
[26] Sohn Won Joon, Lim Jeffrey, Wang Po T, Pu Haoran, Malekzadeh-Arasteh Omid, Shaw Susan J, Armacost Michelle, Gong Hui, Spencer Kellis, Andersen Richard A, others. Bench-top and bedside validation of a low-cost programmable cortical stimulator in a testbed for bi-directional brain-computer-interface research. Front Neurosci 2022;16. Pub-lisher: Frontiers Media SA.
[27] Kuncel Alexis M, Grill Warren M. Selection of stimulus parameters for deep brain stimu-lation. Clin Neurophysiol November 2004;115(11):2431–41.
[28] Wang Po T, Camacho Everardo, Wang Ming, Li Yongcheng, Shaw Susan J, Armacost Michelle, Gong Hui, Kramer Daniel, Lee Brian, Andersen Richard A, others. A benchtop system to assess the feasibility of a fully independent and implantable brain-machine interface. J Neural Eng 2019;16(6):066043. Publisher: IOP Publishing.
[29] Wang PT, King CE, Shaw SJ, Millett DE, Liu CY, Chui LA, Nenadic Z, Do AH. A co-registration approach for electrocorticogram electrode localization using post-implantation MRI and CT of the head. In: Neural engineering (NER), 2013 6th international IEEE/EMBS conference on. IEEE; 2013. p. 525–8.
[30] Lim Jeffrey, Wang Po T, Shaw Susan J, Gong Hui, Armacost Michelle, Liu Charles Y, Do An H, Heydari Payam, Nenadic Zoran. Artifact propagation in subdural cortical electrostimulation: characterization and modeling. Front Neurosci 2022;16. Publisher: Frontiers Media SA.
[31] Klein S, Staring M, Murphy K, Viergever MA, Pluim JPW. Elastix: a toolbox for intensity-based medical image registration. IEEE Trans Med Imag 2010;29(1):196–205. Publisher: IEEE.
[32] Shamonin DP, Bron EE, Lelieveldt BPF, Smits M, Klein S, Staring M. Fast parallel image registration on CPU and GPU for diagnostic classification of Alzheimer's disease. Front Neuroinf 2014;7:50. Publisher: Frontiers.
[33] Das Koel, Nenadic Zoran. An efficient discriminant-based solution for small sample size problem. Pattern Recogn 2009;42(5):857–66. Publisher: Elsevier.
[34] Nicolelis Miguel AL, Alho Eduardo JL, Donati Ana RC, Yonamine Seidi, Aratanha Maria A, Bao Guillaume, Campos Debora SF, Almeida Sabrina, Fischer Dora, Shokur Solaiman. Training with noninvasive brain–machine interface, tactile feedback, and locomotion to en-hance neurological recovery in individuals with complete paraplegia: a randomized pilot study. Sci Rep 2022;12(1):20545.
[35] Chandrasekaran Santosh, Nanivadekar Ameya C, McKernan Gina, Helm Eric R, Boninger Michael L, Collinger Jennifer L, Gaunt Robert A, Fisher Lee E. Sensory restoration by epidural stimulation of the lateral spinal cord in upper-limb amputees. eLife 2020;9:e54349.
[36] Sohn Won Joon, Lim Jeffrey, Wang Po T, Shaw Susan J, Armacost Michelle, Gong Hui, Lee Brian, Lee Darrin, Heydari Payam, Andersen Richard A, et al. Early assessment of artificial lower extremity sensory response times and proprioceptive acuity via sensory cortex electrical stimulation. arXiv preprint arXiv:2505 22691 2025.
[37] Levy Robert M, Harvey Richard L, Kissela Brett M, Winstein Carolee J, Lutsep Helmi L, Parrish Todd B, Cramer Steven C, Venkatesan Lalit. Epidural electrical stimulation for stroke rehabilitation: results of the prospective, multicenter, randomized, single-blinded everest trial. Neurorehabilitation Neural Repair 2016;30(2):107–19.
[38] Zhou A, Johnson BC, Muller R. Toward true closed-loop neuromodulation: artifact-free recording during stimulation. Curr Opin Neurobiol 2018;50:119–27. Publisher: Elsevier.
[39] Weiss Jeffrey M, Flesher Sharlene N, Franklin Robert, Collinger Jennifer L, Gaunt Robert A. Artifact-free recordings in human bidirectional brain–computer interfaces. J Neural Eng 2018;16(1):016002.
[40] Lim Jeffrey, Wang Po T, Bashford Luke, Kellis Spencer, Shaw Susan J, Gong Hui, Armacost Michelle, Heydari Payam, Do An H, Andersen Richard A, et al. Suppression of cortical electrostimulation artifacts using pre-whitening and null projection. J Neural Eng 2023;20(5):056018.
[41] Pu H, Lim J, Kellis S, Liu CY, Andersen RA, Do AH, Heydari P, Nenadic Z. Optimal artifact suppression in simultaneous electrocorticography stimulation and recording for bi-directional brain-computer interface applications. J Neural Eng 2020;17(2):026038. Publisher: IOP Publishing.
[42] Flesher Sharlene N, Downey John E, Weiss Jeffrey M, Hughes Christopher L, Herrera Angelica J, Tyler-Kabara Elizabeth C, Boninger Michael L, Collinger Jennifer L, Gaunt Robert A. A brain-computer interface that evokes tactile sensations improves robotic arm control. Science 2021;372(6544):831–6.
[43] Cramer Steven C, Lastra Lindsey, Lacourse Michael G, Cohen Michael J. Brain motor system function after chronic, complete spinal cord injury. Brain 2005;128(12):2941–50.
[44] King Christine E, Wang Po T, McCrimmon Colin M, Chou Cathy CY, Do An H, Nenadic Zoran. The feasibility of a brain-computer interface functional electrical stimulation system for the restoration of overground walking after paraplegia. J NeuroEng Rehabil 2015;12(1):1–11. Publisher: Springer.
[45] Wang Po T, McCrimmon Colin M, King Christine E, Shaw Susan J, Millett David E, Gong Hui, Chui Luis A, Liu Charles Y, Nenadic Zoran, Do An H. Characterization of electrocorticogram high-gamma signal in response to varying upper extremity movement velocity. Brain Struct Funct 2017;222(8):3705–48.
[46] Malekzadeh-Arasteh Omid, Pu Haoran, Lim Jeffrey, Liu Charles Yu, Do An H, Nenadic Zoran, Heydari Payam. An energy-efficient CMOS dual-mode array architecture for high-density ECoG-based brain-machine interfaces. IEEE Trans Biomed Circ Syst 2019;14(2):332–42. Publisher: IEEE.
[47] Malekzadeh-Arasteh Omid, Pu Haoran, Danesh Ahmad Reza, Lim Jeffrey, Wang Po T, Liu Charles Y, Do An H, Nenadic Zoran, Heydari Payam. A fully-integrated 1μW/Channel dual-mode neural data acquisition system for implantable brain-machine

Interfaces. In: 2021 43rd annual international conference of the IEEE engineering in medicine & biology society (EMBC). IEEE; 2021. p. 5780–3.

[48] Pu Haoran, Danesh Ahmad Reza, Malekzadeh-Arasteh Omid, Sohn Won Joon, Do An H, Nenadic Zoran, Heydari Payam. A 40v voltage-compliance 12.75 ma maximum-current multipolar neural stimulator using time-based charge balancing technique achieving 2mv precision. In: 2021 IEEE custom integrated circuits conference (CICC). IEEE; 2021. p. 1–2.

[49] Pu Haoran, Malekzadeh-Arasteh Omid, Danesh Ahmad Reza, Nenadic Zoran, Do An H, Heydari Payam. A CMOS dual-mode brain–computer interface chipset with 2-mV precision time-based charge balancing and stimulation-side artifact suppression. IEEE J Solid State Circ 2021;57(6):1824–40. Publisher: IEEE.